

This work was written as part of one of the author's official duties as an Employee of the United States Government and is therefore a work of the United States Government. In accordance with 17 U.S.C. 105, no copyright protection is available for such works under U.S. Law.

Public Domain Mark 1.0

<https://creativecommons.org/publicdomain/mark/1.0/>

Access to this work was provided by the University of Maryland, Baltimore County (UMBC) ScholarWorks@UMBC digital repository on the Maryland Shared Open Access (MD-SOAR) platform.

Please provide feedback

Please support the ScholarWorks@UMBC repository by emailing scholarworks-group@umbc.edu and telling us what having access to this work means to you and why it's important to you. Thank you.

Spectral indices to monitor nitrogen-driven carbon uptake in field corn

Lawrence A. Corp
Elizabeth M. Middleton
Petya E. Campbell
K. Fred Huemmrich
Craig S.T. Daughtry
Andrew Russ
Yen-Ben Cheng

Spectral indices to monitor nitrogen-driven carbon uptake in field corn

Lawrence A. Corp,^a Elizabeth M. Middleton,^b Petya E. Campbell,^c
K. Fred Huemmrich,^c Craig S.T. Daughtry,^d Andrew Russ,^d Yen-Ben Cheng^e

^aSigma Space Corporation, Lanham, Maryland 20706, USA

^bBiospheric Sciences Branch, NASA/GSFC, Greenbelt, Maryland 20771, USA

^cJoint Center for Earth Systems Technology, UMBC, Baltimore, Maryland 21250, USA

^dHydrology & Remote Sensing Laboratory, USDA ARS, Beltsville, Maryland, 20705, USA

^eEarth Resources Technology Inc., Annapolis Junction, Maryland 20701

Abstract. Climate change is heavily impacted by changing vegetation cover and productivity with large scale monitoring of vegetation only possible with remote sensing techniques. The goal of this effort was to evaluate existing reflectance (R) spectroscopic methods for determining vegetation parameters related to photosynthetic function and carbon (C) dynamics in plants. Since nitrogen (N) is a key constituent of photosynthetic pigments and C fixing enzymes, biological C sequestration is regulated in part by N availability. Spectral R information was obtained from field corn grown at four N application rates of 0, 70, 140, 280 kg N/ha. A hierarchy of spectral observations were obtained: leaf and canopy with a spectral radiometer; aircraft with the AISA sensor; and satellite with EO-1 Hyperion. A number of spectral R indices were calculated from these hyperspectral observations and compared to geo-located biophysical measures of plant growth and physiological condition. Top performing indices included the R derivative index D_{730}/D_{705} and the normalized difference of R_{750} vs. R_{705} (ND_{705}), both of which differentiated three of the four N fertilization rates at multiple observation levels and yielded high correlations with these carbon parameters: light use efficiency (LUE); C:N ratio; and crop grain yield. These results advocate the use of hyperspectral sensors for remotely monitoring carbon cycle dynamics in managed terrestrial ecosystems.

Keywords: remote sensing, vegetation, reflectance, carbon, nitrogen.

1 INTRODUCTION

With the changing climate, there is a need to understand the dynamics of CO₂ uptake by ecosystems as they cycle through seasonal changes and respond to variable environmental conditions such as water, temperature, and light and nutrient availability [1,2]. Terrestrial ecosystems absorb approximately 120 Gt of carbon (C) annually through the physiological process of photosynthesis [3]. This biological C sequestration process is influenced by nitrogen (N) availability, since N is a key component in photochemical enzymes and light harvesting pigments. Gross primary production (GPP) is the net effect of photosynthetic carboxylation and photorespiration processes and is a measure of an ecosystem's ability to capture and store C. GPP can be described as a function of the amount of absorbed photosynthetically active radiation (aPAR) and the efficiency by which vegetation converts aPAR into biomass: $GPP = \epsilon * aPAR$. The gross photosynthetic light use efficiency (LUE) term (ϵ) reflects the maximum unstressed efficiency achieved by the photosynthetic apparatus. In ecosystem LUE process models, remote sensing data are used to provide estimates of the fraction of aPAR ($faPAR$), typically through relationships to spectral indexes such as NDVI [4]. If $faPAR$ and incident PAR can be estimated using satellite data, then the remaining unknown variable is ϵ .

Remote sensing offers a unique opportunity to monitor ecosystems at synoptic time and space scales through observation and understanding of ecosystem carbon-related spectral responses [5]. Large scale monitoring of vegetation characteristics are only possible with remote sensing systems that rely heavily on passive reflectance (R) information. The Hyperspectral-InfraRed Imager (HyspIRI) mission defined by the 2007 NRC Decadal Survey [6] identifies the need for a near term space-borne imaging spectrometer to globally map early signs of ecosystem change through altered physiology. The primary instrument proposed for the HyspIRI mission is a hyperspectral mapper with a 19 day global revisit, which will enable imaging spectroscopy with high temporal repeat to capture the impact of environmental perturbations on ecosystem productivity. Recent advances in airborne hyperspectral imaging systems (i.e., AVIRIS [7], AISA [Specim, Oulu, Finland]) along with the Hyperion instrument on the EO-1 satellite have made it possible to obtain high resolution spatial and full range visible (VIS) to short wave infrared (SWIR) spectral information. These data can be further employed to explore vegetation productivity and changes in both agricultural and surrounding ecosystems, and contribute to further define algorithms and products applicable to the HyspIRI mission. From hyperspectral data, numerous spectroscopic approaches have been developed to utilize features in vegetation spectral curves for biophysical parameters, to distinguish vegetation species and various physiological conditions and phenological stages [8,9,10].

Several algorithms have been proposed to detect changes in chemical composition, including the amount of chlorophyll (Chl), tissue water content, and the amount of lignin, cellulose, and N using hyperspectral remote sensing data [11-23]. Photosynthetic vs. non-photosynthetic canopy fractions can be distinguished using high spectral resolution data and radiative transfer models [24]. Crop species under N augmentations show that certain red edge reflectance indices perform consistently well for photosynthetic parameters but require narrow, high fidelity spectral bands, such that few current satellite sensors can be utilized. Therefore, the scientific fidelity necessary for operational use of spectral indices to estimate ecosystem ϵ has not been established. Nevertheless, the need for a remotely acquired direct spectral method to monitor ϵ (or GEP) is important. Improvements in the direct remote sensing measurement of ϵ with satellite high resolution spectral observations would reduce the uncertainties introduced by current approaches. This research evaluated published vegetation R indices and demonstrated successful methods to apply this information at leaf, canopy and ecosystem scales to provide more accurate assessments of GPP in corn. The specific objective of this study was to compare the ability of R indices at several observation levels to discriminate among experimental treatments and identify relationships to biophysical manifestation of N driven C uptake.

2 MATERIALS AND METHODS

The experiment site, located at USDA Beltsville Agricultural Research Center, is part of an intensive multi-disciplinary project, Optimizing Production Inputs for Economic and Environmental Enhancement (OPE3). An intensive ground sampling protocol was initiated in 2001 across the N test site and within an adjacent wooded riparian wetland. The corn N test site consists of twelve 20 m x 20 m plots large enough to capture the spatial variability of crop and soil parameters with treatment groups of 280, 140, 70, and 0 kg N / ha, which provided a substantial range in plant growth conditions. Leaf and crop biophysical parameters along with canopy R were acquired at the grain fill (R3) reproductive stage. Leaf level measurements included pigment contents, optical properties, total C:N, and maximum photosynthetic rate (A_{max}). Leaf measurements from 2001 to 2007 occurred *in situ* where possible, otherwise uppermost fully expanded leaves (3rd leaf from terminal) were excised from the plant canopy. *In situ* geo-referenced canopy measurements were comprised of leaf area index (LAI), light use efficiency (LUE, ϵ), grain yield (kg/ha), and canopy R.

2.1 Biophysical Observations

Leaf photosynthetic capacity (A_{\max}) was determined *in situ* with the LI-6400 photosynthetic system (LI-COR Biosciences, Lincoln, NE). A_{\max} was determined under controlled conditions of $1660 \mu\text{mol m}^{-2} \text{s}^{-1}$ PAR, saturating CO_2 concentration (1000 ppm), controlled leaf temperature (22°C), and relative humidity ($\sim 35\%$). LUE was calculated as the ratio of C secured by vegetation per unit of absorbed photosynthetic active radiation ($a\text{PAR}$) as determined from leaf optical properties with an ASD spectral radiometer (FieldSpec Pro, Analytical Spectral Devices, Inc., Boulder, CO) coupled to the LI-1800 Integrating sphere. Canopy values were estimated with the gas exchange calculator (GXC), a comprehensive leaf/canopy gas exchange model that used key environmental variables such as LAI, PAR, CO_2 , air temperature, relative humidity, wind speed, and soil moisture on corn to scale from the leaf A_{\max} observations to canopy gas exchange A_{net} [24]. The canopy fraction of absorbed PAR ($f_a\text{PAR}_c$) was derived from LAI measurements using the Beer-Lambert law with the light extinction coefficient k set to 0.55. Grain yields were obtained with a yield monitor (AgLeader 2000, Roswell, GA) measuring the grain flow from the combine at harvest interfaced with a differential GPS.

2.2 Spectral Reflectance

The ASD spectral radiometer was also used to measure canopy radiance 1 m above plant canopies with a 22° field of view and a 0° nadir view zenith angle. A second cross-calibrated ASD radiometer was used in a similar viewing geometry over a Spectralon reference panel (Labsphere, North Sutton, NH) to simultaneously track changes in solar irradiance. The ASD VNIR spectrometer covers the range between 350 – 1000 nm with a 512 channel silicon photodiode array overlaid with an order separation filter to provide a 3 nm Full-Width at Half Maximum (FWHM) spectral resolution with a 1 nm sampling interval. Two separate, thermal electrically cooled InGaAs photodiodes are used to cover the NIR/SWIR range between 1000 - 2500 nm at a 10 nm FWHM spectral resolution. Measurements were obtained on a clear day in a two-hour window around solar noon yielding an average PPFD of $1660 \mu\text{mol m}^{-2} \text{s}^{-1}$. Aircraft multispectral R imagery was acquired on 8-22-2001 and 8-31-2004 with the Airborne Imaging Spectrometer for Applications (AISA, flown by 3DI LLC, Easton MD). The configuration of the AISA imaging spectrometer during this time period was limited to 35 narrow bands between 420 nm to 884 nm. The instrument was flown at 2,500 m with an instantaneous field of view of 1 mrad, yielding a 2.5 m per pixel ground resolution. Hyperspectral satellite data over the study site was acquired on 8-19-2008 with EO-1 Hyperion with 10 AM overpass and a 30 m ground resolution. The Hyperion Level 1R data product has 220 contiguous radiometrically corrected 10 nm FWHM spectral bands covering the spectral range from 400-2500 nm.

2.3 Computation of R Spectral Indices

A number of R indices were evaluated based on two criteria: consistent performance over all measurement scales, and reproducible correlations to biophysical measures of plant growth and condition. The equations defining top performing R indices are summarized in Table 1. These equations were applied to R spectra at all observation levels. A Gaussian 1 nm FWHM spectral resampling procedure was applied to the AISA multispectral imagery to provide a contiguous spectrum over the wavelength range of 500 to 900 nm. Due to the discrete characteristic of the spectral sampling interval, spectral derivatives were expressed as $D_\lambda = (R_{\lambda+1} - R_{\lambda-1}) / \Delta\lambda$, where λ corresponds to the reported wavelength and $\lambda \pm 1$ is governed by the native spectral sampling interval.

Table 1. Reflectance spectral indices identified as exhibiting significant relationships to corn growth and condition at three observation levels: leaf, canopy, and aircraft.

Spectral Index	Reference
$CI_{red-edge} = (R_{770-800}/R_{720-730})-1$	Gitelson et al., 2004
$CRI_{550} = (1/R_{510})-(1/R_{550})$	Gitelson et al., 2002
D_{730}/D_{705}	
D_{max}/D_{705}	Filella & Penuelas 1994
D_{max}/D_{744}	Curran et al., 1995
$EVI = 2.5(R_{840-875} - R_{620-670})/(R_{840-875} + 6R_{620-670} + 1)$	Huete et al., 2002
$MCARI_b = [(R_{700}-R_{630})-0.23(R_{700}-R_{550})](R_{700}/R_{630})$	Daughtry et al., 2000
$ND_{705} = (R_{750}-R_{705})/(R_{750}+R_{705})$	Simms & Gammon 2002
$mND_{705} = (R_{750}-R_{705})/(R_{750}+R_{705}-2R_{445})$	Simms & Gammon 2002
$NDVI = (R_{774}-R_{667})/(R_{774}+R_{667})$	Tucker 1979
$PRI_{550} = (R_{550}-R_{531})/(R_{550}+R_{531})$	Gammon et al., 1992
R_{705}/R_{930}	Read et al., 2002
R_{750}/R_{705}	Gitelson et al., 1994
R_{740}/R_{720}	Vogelman et al., 1993
R_{750}/R_{550}	Gitelson et al., 1994
R_{800}/R_{750}	
R_{860}/R_{550}	Datt et al., 1998
$TCARI = 3[(R_{700}-R_{670})-0.2(R_{700}-R_{550})(R_{700}/R_{670})]$	Haboudane et al., 1995
$VOG = (R_{734}-R_{747})/(R_{715}+R_{720})$	Vogelman et al., 1993

3 RESULTS

3.1 Biophysical Summary of Field Corn Growth

Multi-year analysis (2001 to 2007) of field corn growth indicated that values for leaf variables (Chl, N, ϵ_L) and crop variables ($\hat{a}PAR_C$, ϵ_C , grain yield) increased with N level (Table 2). Foliar N content increased with application rate, with the ANOVA model successfully discriminating the four treatment levels at a minimum significant difference of 0.084 g m⁻². For the remaining foliar variables (Chl, C:N, and ϵ_L) and the three canopy variables ($\hat{a}PAR_C$, ϵ_C , grain yield), similar values were obtained for the N treatment groups ≥ 140 kg N/ha which were significantly higher than values observed for treatments ≤ 70 kg N/ha. The GXC model provided good agreement between measured and observed ϵ_L with a slightly higher bias in the modeled parameter. Further LUE increases were incurred by the inclusion of all leaf layers in the GXC scaling from ϵ_L to ϵ_C . Overall, the analysis of corn growth and condition indicates the recommended N application rate of 140 kg N /ha was optimal for corn grown at this location on a sandy loam soil, while lowering the application rate produced crop symptoms consistent with N deficiency.

Table 2. Multi-year analysis of leaf and canopy biophysical parameters as a function N application rate.

Application (kg N/ha)	Chl (g/m ²)	N (g/m ²)	C:N	$\epsilon_{\text{Leaf}}^{\#}$	$faPAR_C$	$\epsilon_{\text{Canopy}}^{\#}$	Yield (Mg/ha)
280	0.58 a [†]	1.97 a	14.9 a	0.34 a	0.77 a	0.62 a	7.23 a
140	0.55 a	1.88 b	15.8 a	0.33 a	0.76 a	0.61 a	7.10 a
70	0.48 b	1.62 c	17.8 b	0.31 b	0.73 b	0.57 b	5.94 b
0	0.29 c	1.12 d	25.6 c	0.22 c	0.64 c	0.39 c	3.78 c
LSD _{.05}	0.025	0.084	1.04	0.014	0.016	0.023	0.277

[†]Column-wise mean values (n=265) represent analysis corn growth parameters taken in the reproductive development stages from 2001 to 2007. Means with the same letter are not separable by a repeated measures mixed model ANOVA_{LSD,05}. [#]Leaf and canopy light use efficiency (ϵ) are expressed as $\mu\text{g C per } \mu\text{mol of absorbed photosynthetically active radiation (aPAR)}$.

3.2 Spectral Remote Sensing of C Parameters with Reflectance

Spectral index performance was evaluated against measures of plant growth condition using correlation analysis. Results for the top performing indices exhibiting strong relationships to LUE, C:N and grain yield across years are shown in Table 3. All of these indices showed good correlation ($r > 0.70$) to at least one leaf, canopy, or aircraft variable. Since the columns for the three biophysical assessments were obtained on excised leaf material with a laboratory based spectrometer attached to an integrating sphere, reported relationships are solely attributed to variations in leaf chemical and structural composition. Whereas for canopy and aircraft observations, variations were due to many factors including; light history, bi-directional R distributions, and canopy structure, which have impacts on the observed relationships. The highest association was obtained with the derivative index D_{max}/D_{744} in the near-field canopy R observations for C:N ($r = 0.90$) and LUE ($r = -0.88$). The fixed wavelength derivative index D_{730}/D_{705} also performed well with consistently high correlations for all three variables across measurement scales ($0.75 > r > 0.85$). NDVI, historically being associated with canopy biomass, performed as expected with relatively poor leaf level physiological associations, which significantly improved for canopy and aircraft observations.

For this study, the ND_{705} index provided higher correlations and more consistent results than the more traditional NDVI formulation, and was similar in performance to D_{730}/D_{705} across variables and measurement scale ($0.70 > r > 0.82$). The PRI_{550} , which is commonly used as a remotely sensed indicator of LUE in plant canopies, performed moderately well ($0.68 > r > 0.74$) at the leaf and aircraft levels but was ineffective in the near canopy observations. At the ASD near-field canopy observation level, the D_{730}/D_{705} and ND_{705} spectral indices performed well in detecting N treatment level with minimum significant index differences of 0.108 and 0.019 respectively [In 24, Table 4b]. At the AISA aircraft observation level these two spectral R indices differentiated the four N application rates [In 24, Table 4c]. These observations imply that N induced changes in leaf physiology combined with changes in canopy structure ($faPAR$, Table 2) contributed to improved index performance when scaling from leaf to aircraft observation levels.

3.3 Spatial Analysis of Crop Condition

The ND_{705} and D_{730}/D_{705} R images with spatial extent covering the N experiment site at OPE3 along with kriged yield monitor data in a 2 m grid are shown in Fig. 1. The N treatment plots are delineated with a white vector overlay on the geo-coded raster images. Here, spatial associations are evident between each of the two R indexes and yield monitor data with variation induced by N application rates are visually apparent; color bars at the bottom of

Table 3. Pearson correlation coefficients (r, n=265) for the relationship between 19 narrow-band spectral indices and physiological measures of plant growth at leaf (L), near-field canopy (C), and far-field aircraft (AISA) measurement scales.

R Index	LUE [†]			C:N			Yield		
	L	C	AISA	L	C	AISA	L	C	AISA
CI _{red-edge}	0.75*	0.77	0.76	-0.77	-0.81	-0.80	0.75	0.83	0.78
CRI ₅₅₀	-0.82	-0.25	-0.71	0.85	0.20	0.71	-0.80	-0.21	-0.68
D ₇₃₀ /D ₇₀₅	0.75	0.80	0.79	-0.77	-0.84	-0.81	0.79	0.85	0.79
D _{max} /D ₇₀₅	0.66	0.73	0.78	-0.68	-0.77	-0.81	0.71	0.82	0.79
D _{max} /D ₇₄₄	-0.72	-0.88	-0.75	0.73	0.90	0.80	-0.68	-0.73	-0.76
EVI	0.59	0.68	0.76	-0.59	-0.74	-0.79	0.43	0.73	0.77
MCARI _b	-0.73	-0.53	-0.81	0.75	0.53	0.84	-0.73	-0.56	-0.77
ND ₇₀₅	0.74	0.78	0.79	-0.76	-0.82	-0.81	0.70	0.76	0.78
mND ₇₀₅	0.74	0.77	0.79	-0.75	-0.82	-0.81	0.70	0.76	0.78
NDVI	0.27	0.66	0.76	-0.25	-0.71	-0.79	ns	0.62	0.77
PRI ₅₅₀	0.71	0.36	0.73	-0.73	-0.37	-0.74	0.71	0.38	0.68
R ₇₀₅ /R ₉₃₀	-0.76	-0.82	na [#]	0.77	0.85	na	-0.72	-0.79	na
R ₇₅₀ /R ₇₀₅	0.71	0.70	0.76	-0.73	-0.75	-0.78	0.69	0.77	0.78
R ₇₄₀ /R ₇₂₀	0.75	0.76	0.77	-0.77	-0.81	-0.80	0.76	0.81	0.78
R ₇₅₀ /R ₅₅₀	0.72	0.73	0.76	-0.74	-0.78	-0.78	0.64	0.84	0.76
R ₈₀₀ /R ₇₅₀	0.72	0.74	0.75	-0.73	-0.76	-0.80	0.78	0.86	0.76
R ₈₆₀ /R ₅₅₀	0.73	0.74	0.76	-0.74	-0.79	-0.79	0.66	0.87	0.76
TCARI	-0.73	-0.54	-0.82	0.75	0.56	0.83	-0.66	-0.60	-0.77
VOG	-0.74	-0.74	-0.77	0.76	0.78	0.80	-0.76	-0.82	-0.78

[†]Midday light use efficiency was used for leaf (ϵ_l) while for canopy and aircraft observations the GXC scaled ϵ_c was used. *Except for low correlation between leaf-level NDVI and yield, r values were significant at $P < 0.01$. [#]Band not available (na).

each panel depict the magnitude of variation, where black is associated with low and yellow indicating high index or yield values. Observed within-plot variation is attributed to variable soil and hydrological properties. Overall, the low N application rates are evidenced by blue-green hues while the high N application rates are indicated by red-yellow hues.

The relationship between LUE and ASD leaf, ASD canopy, AISA aircraft versions of the D₇₃₀/D₇₀₅ and ND₇₀₅ indices were further explored in [In 24, Fig. 6] where observations implied a significant relationship between LUE and early to mid-day R indices. The ND₇₀₅ and D₇₃₀/D₇₀₅ R images with spatial extent covering the entire OPE experiment site along with the yield monitor image delineating the size and extent of the 12 N treatment plots are shown in Fig. 2. Again, color bars at the bottom of each panel indicate the magnitude of variation with black indicating low and yellow indicating high index or yield values. The soil berms delineating the four hydrologically bounded watersheds are visible in the imagery as low index and yield values. Variation is evident with spatial associations between yield monitor and R indices apparent in several clusters of low and high performing areas of the field.

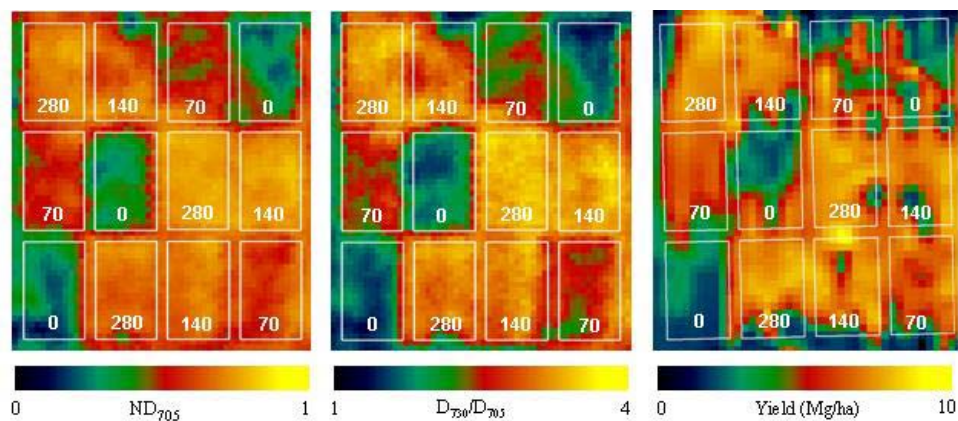


Fig. 1. Reflectance normalized difference (left) and reflectance derivative ratio (middle) spectral indices along with yield monitor data (right) for the 12 N treatment plots located at the OPE field site as determined from AISA 2004 multispectral imagery.

One more observation level was added by including Hyperion satellite data. The relationships between yield monitor data and R indices determined from ASD, AISA aircraft, and Hyperion R for D_{730}/D_{705} and ND_{705} were further explored in Fig. 3. The left most scatter plots indicate the association of near field canopy ASD R index observations to yield monitor data extracted from the 12 N treatment plots across multiple years ($n=265$, corresponding to area shown in Fig. 1). The scatter plots in the center and to the right show the respective associations for these two indices computed from aircraft (AISA 2004, $n=1920$ pixels) and satellite (Hyperion 2008, $n=335$ pixels) to yield monitor data for the full OPE field site.

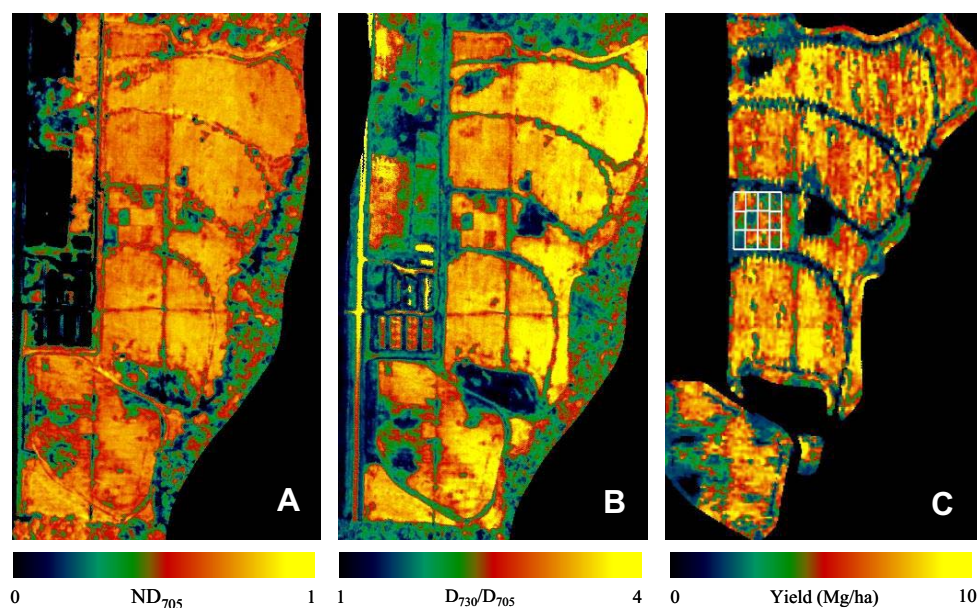


Fig. 2. Reflectance normalized difference (A) and reflectance derivative ratio (B) spectral indices along with yield monitor data (C) over the entire 4 ha OPE field site as viewed from AISA multispectral imagery. Note location of the 12 400 m² N plots in C.

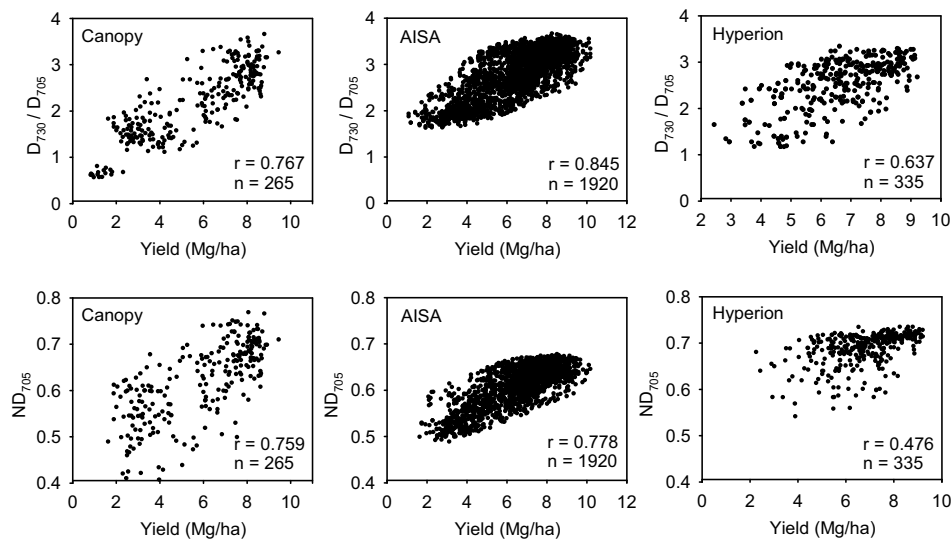


Fig. 3. Reflectance derivative ratio (top) and reflectance normalized difference (bottom) spectral indices versus yield monitor data over the OPE field site.

The direct linear association ($0.63 < r < 0.85$) between grain yield and the derivative ratio D_{730}/D_{705} was expressed at all three remote sensing observation levels, where index values were ~ 1 for low performing areas of the field and approached 4 for areas with high grain yield. A similar pattern was observed for the ND₇₀₅ but the index exhibited more noise which reduced correlation coefficients ($0.47 < r < 0.78$). These early to mid-day remote sensing observations made of a corn canopy in the early reproductive growth phases express a significant relationship to grain yields obtained for the mature crop at harvest.

4 DISCUSSION

From this study, a number of significant relationships were evident in R indices to the biophysical changes in corn induced by varying N application rates. High spectral resolution reflectance data have provided significant improvement over the broadband indices for detection of differences in vegetation physiology. Further relationships between R and vegetative growth parameters have also been achieved with several derivative leaf R indices. However, the spectral sampling resolution of the AISA instrument was not sufficient to accurately identify the wavelength position of D_{\max} or identify a significant red-edge shift in N limiting environments. However, the shift was observed in 10 nm FWHM continuous hyperspectral sampling of AVIRIS and Hyperion, reinforcing the importance of continuous sampling versus spectral resolution for applications involving derivative spectroscopy. The recent advances in airborne hyperspectral imaging systems (i.e., AISA EAGLE & Hawk) along with the steady progress of the AVIRIS group [7] have made it possible to obtain high resolution spatial and full range VIS to SWIR spectral information that should be further employed to explore the impact of N availability on vegetative C uptake in both agricultural and natural ecosystems.

Timely, spatially explicit information can provide input into decisions about management of agriculture and other ecosystems to mitigate negative effects. The observations would also underpin improved scientific understanding of ecosystem responses to climate change and management, which ultimately supports climate modeling and forecasting capabilities. Vegetation change, in turn, feeds back into the understanding, prediction, and mitigation of factors that drive climate change. The HypsIRI mission defined by the NRC Decadal Survey

[6] identifies the need for a space-borne VSWIR hyperspectral imaging spectrometer for global surveys, especially to detect early signs of ecosystem change. The proposed HypsIRI mission with its global mapping capability at a 19 day revisit will enable hyperspectral imaging spectroscopy to capture the impact of disturbance events on ecosystem LUE seasonally. The findings achieved here with EO-1 Hyperion demonstrate the utility of space-borne imaging spectroscopy to monitor ecosystem carbon exchange and LUE.

5 CONCLUSIONS

Here multiple years of spectral observations of field corn made at leaf, canopy, aircraft, and satellite observation levels were used to: identify spectral R indices that consistently track biophysical changes in field corn indicative of productivity; establish spectral R index performance across observation levels and through time; provide a synopsis of top performing spectral indices to monitor N driven C dynamics in field corn. Results presented here indicate significant relationships exist between narrow band spectral R indices to C related vegetation parameters. These results strongly support the application of high resolution imaging spectrometers for remotely monitoring carbon cycle dynamics in terrestrial ecosystems and provide critical information to define the optimal narrow bands required for monitoring ecosystem health from earth-orbiting satellites.

References

- [1] J.L. Sarmiento, and S.C. Wofsy, A U.S. Carbon Cycle Science Plan, *A Report of the Carbon and Climate Working Group of the U.S. Global Change Research Program*, 69 pp. (1999).
- [2] G.R. Walther, E. Post, P. Convey, A. Menzel, C. Parmesan, T.J.C. Beebee, J.M. Fromentin, O. Hoegh-Guldberg, and F. Bairlein, "Ecological responses to recent climate change," *Nature* **416**(6879): 389-395(2002) [[doi:10.1038/416389a](https://doi.org/10.1038/416389a)].
- [3] H.H. Janzen, "Carbon cycling in earth systems - a soil science perspective," *Agriculture, Ecosystems & Environment* **104**, 399-417 (2004) [[doi:10.1016/j.agee.2004.01.040](https://doi.org/10.1016/j.agee.2004.01.040)].
- [4] K. F. Huemmrich, and S. N. Goward, "Vegetation canopy PAR absorptance and NDVI: an assessment for ten tree species with the SAIL model," *Remote Sens. Environ.* **61** (2): 254-269 (1997) [[doi:10.1016/S0034-4257\(97\)00042-4](https://doi.org/10.1016/S0034-4257(97)00042-4)].
- [5] A. F. H. Goetz, G. Vane, J. E. Solomon, and B. N. Rock, "Imaging Spectrometry For Earth Remote-Sensing," *Science* **228**, 1147-1153 (1985) [[doi:10.1126/science.228.4704.1147](https://doi.org/10.1126/science.228.4704.1147)].
- [6] Space Studies Board of the National Research Council, "Earth Science and Applications from Space: National Imperatives for the Next Decade and Beyond," pp. 113-115, *The National Academies Press*, Washington D.C., 2007.
- [7] R.O. Green, M.L. Eastwood, C.M. Sarture, T.G. Chrien, M. Aronsson, B.J. Chippendale, J.A. Faust, B.E. Pavri, C.J. Chovit, M. Solis, M.R. Olah, O. Williams, "Imaging Spectroscopy and the Airborne Visible/Infrared Imaging Spectrometer (AVIRIS)," *Remote Sens. Environ.* **65**(3) 227-248 (1998) [[doi:10.1016/S0034-4257\(98\)00064-9](https://doi.org/10.1016/S0034-4257(98)00064-9)].
- [8] G. P. Asner, "Biophysical and biochemical sources of variability in canopy reflectance," *Remote Sens. Environ.*, **64**, 234-253 (1998) [[doi:10.1016/S0034-4257\(98\)00014-5](https://doi.org/10.1016/S0034-4257(98)00014-5)].
- [9] P.K. Entcheva, B.N. Rock, M. Martin, C. Neefus, J. Irons, E.M. Middleton and J. Albrechtova, "Detection of initial damage in Norway spruce canopies using high spectral resolution airborne data," *Int. J. Remote Sens.* **25**: 24, 5557-5583 (2004) [[doi:10.1080/01431160410001726058](https://doi.org/10.1080/01431160410001726058)].

- [10] E.M. Middleton, Y.-B. Cheng, T. Hilker, T.A. Black, P. Krishnan, N.C. Coops, and K.F. Huemmrich, "Linking Foliage Spectral Responses to Canopy Level Ecosystem Photosynthetic Light Use Efficiency at a Douglas-fir Forest in Canada," *Canadian Journal of Remote Sensing*, **35**:2, 166-188, (2009).
- [11] A.A. Gitelson, and M. N. Merzlyak, "Non-destructive assessment of chlorophyll, carotenoid and anthocyanin content in higher plant leaves: Principles and algorithms," *Remote Sensing for Agriculture and the Environment*, S. Stamatiadis, J.M. Lynch, J.S. Schepers Eds., Greece, Ella, pp. 78-94 (2004).
- [12] I. Filella, and J. Pen˜uelas, "The red edge position and shape as indicators of plant chlorophyll content, biomass and hydric status," *Int. J. Remote Sens.* **15**:7, 1459–1470 (1994) [[doi:10.1080/01431169408954177](https://doi.org/10.1080/01431169408954177)].
- [13] P.J. Curran, W.R. Windham, and H.L. Gholz, "Exploring the Relationship Between Reflectance Red Edge and Chlorophyll Concentration in Slash Pine Leaves," *Tree Physiol.* **15**:203-206 (1995).
- [14] A. Huete, K. Didan, T. Miura, E.P. Rodriguez, X. Gao, and L.G. Ferreira, "Overview of the radiometric and biophysical performance of the MODIS vegetation indices," *Remote Sens. Environ.* **83**, 195–213 (2002) [[doi:10.1016/S0034-4257\(02\)00096-2](https://doi.org/10.1016/S0034-4257(02)00096-2)].
- [15] C.S.T. Daughtry, C.L. Walthall, M.S. Kim, E. Brown de Colstoun, J.E. McMurtrey, "Estimating corn leaf chlorophyll concentration from leaf and canopy reflectance," *Remote Sens. Environ.* **74**:229-239 (2000) [[doi:10.1016/S0034-4257\(00\)00113-9](https://doi.org/10.1016/S0034-4257(00)00113-9)].
- [16] D.A. Sims, J.A. Gamon, "Relationship between leaf pigment content and spectral reflectance across a wide range species, leaf structures and development stages," *Remote Sens. Environ.* **81**: 337–354 (2002) [[doi:10.1016/S0034-4257\(02\)00010-X](https://doi.org/10.1016/S0034-4257(02)00010-X)].
- [17] C.J. Tucker, "Red and Photographic Infrared Linear Combinations for Monitoring Vegetation," *Remote Sens. Environ.* **8**:127-150, (1979) [[doi:10.1016/0034-4257\(79\)90013-0](https://doi.org/10.1016/0034-4257(79)90013-0)].
- [18] J.A. Gamon, L. Serrano, and J.S. Surfus, "The Photochemical Reflectance Index: An Optical Indicator of Photosynthetic Radiation Use Efficiency Across Species, Functional Types and Nutrient Levels," *Oecologia*, **112**:492-501, 1997 [[doi:10.1007/s004420050337](https://doi.org/10.1007/s004420050337)].
- [19] J. J. Read, L. Tarpley, J. M. McKinion, and K. R. Reddy, "Narrow-Waveband Reflectance Ratios for Remote Estimation of Nitrogen Status in Cotton," *J. Environ. Qual.* **31**: 1442-1452 (2002) [[doi:10.2134/jeq2002.1442](https://doi.org/10.2134/jeq2002.1442)].
- [20] A.A. Gitelson, and M. N. Merzlyak, "Quantitative estimation of chlorophyll a using reflectance spectra: Experiments with autumn chestnut and maple leaves," *J. Photochem. Photobiol.* **22**:247–252 (1994) [[doi:10.1016/1011-1344\(93\)06963-4](https://doi.org/10.1016/1011-1344(93)06963-4)].
- [21] J.E. Vogelmann, B.N. Rock, and D.M. Moss, "Red edge spectral measurements in sugar maple leaves," *Int. J. Remote Sens.* **14**(8): 1563-1575 (1993) [[doi:10.1080/01431169308953986](https://doi.org/10.1080/01431169308953986)].
- [22] B. Datt, "Remote sensing of chlorophyll a, chlorophyll b, and total carotenoid content in eucalyptus leaves," *Remote Sens. Environ.* **66**: 111–121 (1998). [[doi:10.1016/S0034-4257\(98\)00046-7](https://doi.org/10.1016/S0034-4257(98)00046-7)]
- [23] D. Haboudane, J. R. Miller, E. Pattey, P. J. Zarco-Tejada, and I. B. Strachan, "Hyperspectral vegetation indices and novel algorithms for predicting green LAI of crop canopies: Modeling and validation in the context of precision agriculture," *Remote Sens. Environ.* **90**:337-352 (2004) [[doi:10.1016/j.rse.2003.12.013](https://doi.org/10.1016/j.rse.2003.12.013)].
- [24] S.H. Kim, R.C. Sicher, H. Bae, D.C. Gitz, J.T. Baker, D.J. Timlin, and V.R. Reddy, "Canopy photosynthesis, evapotranspiration, leaf nitrogen and transcription profiles of maize in response to CO₂ enrichment," *Global Change Biol.* **12**, 588-600 (2006) [[doi:10.1111/j.1365-2486.2006.01110.x](https://doi.org/10.1111/j.1365-2486.2006.01110.x)].